Mercury Export Flux in the Arctic Ocean Estimated from 234 Th/ 238 U Disequilibria

Javier Tesán Onrubia, Mariia Petrova, Viena Puigcorbé, Erin Black, Ole Valk, Aurélie Dufour, Bruno Hamelin, Ken Buesseler, Pere Masqué, Frédéric A.C. Le Moigne, et al.

Paper 'Mercury export flux in the Arctic Ocean estimated from Th^{234}: U^{238} disequilibrium'

Javier A. Tesán Onrubia[1], Mariia V. Petrova[1], Viena Puigcorbé[2], Erin E. Black[3,4], Ole Valk[5], Aurelie Dufour[1], Bruno Hamelin[6], Ken O. Buesseler[7], Pere Masqué[2,8,9], Frederic A.C. Le Moigne[1], Jeroen E. Sonke[10], Michiel Rutgers van der Loeff[5], Lars-Eric Heimbürger-Boavida[1]*

1. Aix Marseille Université, CNRS/INSU, Université de Toulon, IRD, Mediterranean Institute of Oceanography, Marseilles, France
2. School of Science, Centre for Marine Ecosystems Research, Edith Cowan University, Joondalup, WA, Australia.
3. Ocean Frontier Institute - Dalhousie University, Halifax, Canada
4. Lamont-Doherty Earth Observatory, Palisades NY, USA
5. Alfred Wegener Institute Helmholtz Centre for Polar and Marine Research, Bremerhaven, Germany
6. Aix Marseille Université, CNRS, IRD, INRA, Coll France, CEREGE, Aix en Provence, France
7. Woods Hole Oceanographic Institution, Woods Hole, MA, USA
8. Institut de Ciència i Tecnologia Ambientals and Departament de Física, Universitat Autònoma de Barcelona, Cerdanyola del Vallès, Barcelona, Spain.
9. International Atomic Energy Agency, 4a Quai Antoine 1er, 98000 Principality of Monaco, Monaco
10. Laboratoire Géosciences Environnement Toulouse, CNRS/IRD/CNES/Université Paul Sabatier–Toulouse III, France

Corresponding author: lars-eric.heimburger@mio.osupytheas.fr

Abstract

High mercury (Hg) levels have been observed for arctic biota despite limited local sources of anthropogenic Hg in the Arctic. Scavenging of Hg exerts an important control on the residence time of Hg in surface waters. The downward Hg export flux, as well as Hg burial rates in bottom sediments, are not well constrained due to the lack of particulate Hg (pHg) observations in the Arctic Ocean. Here we estimated downward Hg export flux based on Hg concentrations in suspended particulate matter (SPM) and by using the radionuclide pair $^{234}Th/^{238}U$, coupled to $pHg/^{234}Th$ ratios in particles. Using new observations made during the German GEOTRACES TransArcII (GN04) and the U.S. Arctic GEOTRACES (GN01) cruises in August - October 2015, we estimated the pHg export flux in the central Arctic Ocean and the outer shelf. We find that 81 ± 58 Mg y^{-1} pHg are exported from the upper 100 m, of which 16 ± 10 Mg y^{-1} are ultimately buried in marine sediments. An extrapolation to the entire Arctic Ocean, including the inner shelf, results in 156 Mg y^{-1} pHg export from the surface ocean and 28 Mg y^{-1} Hg burial rate. Our study shows that the pHg export flux could be higher than previously thought and this should be taken into consideration for future arctic Hg budget estimations.

Keywords

GEOTRACES, particulate mercury, Arctic Ocean, thorium export, particle export flux

Main text

Elevated Hg levels in arctic biota (Dietz et al., 2013, Wang et al., 2018, Dudarev et al., 2019) have been explained by enhanced inorganic Hg inputs to the Arctic Ocean (Outridge et al., 2008, Fisher et al., 2012). Several recent studies aimed at refining Hg inputs from the atmosphere (Schroeder et al., 1998, Soerensen et al., 2016), rivers (Sonke et al., 2018), coastal erosion (Leitch et al., 2007, Schuster et al., 2019, Lim et al., 2020) and other oceans (Cossa et al., 2018, Petrova et al., 2020). Once delivered to the Arctic Ocean, Hg can undergo complex biotic and abiotic reactions, including the transformation into the bioaccumulative neurotoxin methylmercury (MeHg). Because MeHg is produced at shallow depth in the Arctic Ocean (Heimbürger et al., 2015), it is important to know the residence time of Hg, which is largely driven by two removal mechanisms: evasion to the atmosphere and downward export flux with settling particles.

Due to Hg's high affinity for particles, scavenging and export flux play a major role in removing Hg from the surface ocean (Lamborg et al., 2016). A fraction of this downward Hg export flux is finally buried in the marine sediments and in this way removed from the oceanic Hg budget for millennial time scales. Providing the first comprehensive Arctic Hg budget Outridge et al. (2008) estimated a burial rate of Hg to the marine sediments of 108 Mg y^{-1}. Later on, Soerensen et al. (2016) established a box model which estimates the downward pHg flux to be 37 Mg y^{-1} and a burial rate of 28 Mg y^{-1} based on the few observations available at the time. Both studies also differ in their estimation of the exchange flux with the atmosphere (Tab. S1). Outridge et al. (2008) find a low Hg evasion flux of 10 Mg y^{-1}, which results in a net atmospheric deposition of 98 Mg y^{-1} to the Arctic Ocean. On the contrary the box model developed by Soerensen et al. (2016) implies that the Arctic Ocean is a Hg source with a net evasion flux to the atmosphere of 23 Mg y^{-1}. The downward Hg export flux from the surface to the deep Arctic Ocean, as well as Hg burial rate in marine sediments, remain

poorly constrained (Tab. S1). Sedimentation rates in the central Arctic Ocean are thought to be very low, and sediment mixing and diagenesis bias the Hg sediments records (Gobeil et al., 1999). Most sediment traps deployed in the Arctic Ocean use $HgCl_2$ for sample preservation (Kraft et al., 2013) and cannot be used for Hg analysis. Thus far only one study could provide particulate Hg (pHg) measurements in the central Arctic Ocean (Agather et al., 2019).

Previous estimates of Hg fluxes in the Arctic Ocean (Outridge et al., 2008, Fisher et al., 2012, Soerensen et al., 2016) had to be based on available information of pHg in riverine particles (Graydon et al., 2009), ice algae (Burt et al., 2012) and zooplankton (Pućko et al., 2014), sediments (Macdonald et al., 1991, Gobeil et al., 1999), or by using partition coefficients (K_d) from the North Atlantic (1.1×10^5 L kg^{-1}, Mason et al., 1998) or the Pacific Ocean (1×10^6 L kg^{-1}, Mason et al., 1993). Fisher et al. (2012) used the GEOS-Chem model to explain atmospheric Hg observations in the Arctic. In the absence of pHg observations for the Arctic Ocean, this study used the K_d from the North Atlantic (Mason et al., 1998) to estimate the Hg export flux of 43 Mg y^{-1} in the Arctic Ocean. Typically, the GEOS-Chem model uses an average K_d of 3.2×10^5 L kg^{-1} for simulations in other oceans. A recent study, conducted in the North Atlantic by Lamborg et al. (2016), showed that observed K_d values are an order of magnitude higher (4.5×10^6 L kg^{-1}). Soerensen et al. (2016) conducted a box model study that suggested that about 37 Mg y^{-1} of Hg are exported below 200 m depth. The authors estimated Hg export fluxes based on particulate fluxes of solids from rivers and erosion (660 Tg y^{-1}) and primary production (1,100 Tg y^{-1} of which 35 Tg y^{-1} are exported below 200 m depth). In the absence of pHg data the authors used a best estimate of 50 ng g^{-1} for all types of particles in the Arctic Ocean.

We used new observations, to develop two different approaches to provide a new estimate for the pHg export flux in the central Arctic Ocean and in the outer shelf (> 100 m).

First, we used new data to calculate pHg normalized to suspended particulate matter (Hg_{SPM}) and K_d for the Arctic Ocean. Then, we used pHg and ^{234}Th observations, to estimate the pHg export flux based on the $^{234}Th/^{238}U$ disequilibrium (Coale et al., 1985). Finally, we re-estimated the net Hg burial rates from our Arctic sediment cores. The data we used in this study came from two GEOTRACES cruises in 2015 to the Arctic Ocean and that overlapped at the North Pole. The Barents Sea and the central Arctic Ocean were sampled during the GEOTRACES TransArc II (GN04) cruise between 17th August and 15th October 2015 aboard the FS Polarstern. The Western and central Arctic Ocean were sampled during the U.S. Arctic GEOTRACES (GN01) cruise between 9th August and 12th October 2015. Both ships sampled near the North Pole on 7th September 2015. For the GN04 cruise we measured pHg concentrations on pre-combusted QMA filters (1 - 53µm) mounted on *in situ* pumps deployed at 100 m depth at 9 stations. The station's locations included permanently ice-covered areas in the central Arctic Ocean (stations 32, 50, 81, 96, 101, and 125) as well as ice free stations on the shelf of the Barents Sea (stations 4, 153, and 161; Tab. S2). During the GN01 cruise, Agather et al. (2019) measured pHg concentrations on QMA filters (1 - 51 µm) at 100 m depth at 9 ice-covered stations in the central Arctic Ocean and 1 ice free station on the outer shelf (Tab. S2).

Particulate Hg concentrations on GN04 averaged 0.097 ± 0.039 pmol L^{-1} (n = 9), and are similar those measured in the Western Arctic Ocean during the GN01 cruise (0.072 ± 0.051 pmol L^{-1}, n = 10, Agather et al., 2019), but about 3 times higher than pHg measured in the North Atlantic (Mason et al., 1998, Bowman et al., 2015). The highest pHg concentrations were observed over the shelf (GN04: 0.137 ± 0.046 pmol L^{-1}, n = 3; GN01: 0.204 pmol L^{-1}, n = 1) and lowest off-shore (GN04: 0.076 ± 0.008 pmol L^{-1} n = 6; GN01: 0.058 ± 0.022 pmol L^{-1}, n = 9). The pHg concentrations were converted from water volume (pHg in pmol L^{-1}) to particle mass-specific concentrations (Hg_{SPM} in ng g^{-1}), using SPM

concentrations from the GN01 cruise for each station at depths between 80 and 120 m (Lam et al., 2020). In the absence of SPM measurements on GN04, we applied average values from the GN01 cruise, 9.29 ± 2.28 µg L^{-1} for the central Arctic Ocean and of 146 ± 8.46 µg L^{-1} for the outer shelf (Table S2). The Hg_{SPM} concentrations at 100 m depth were 211 ± 69 ng g^{-1} on the shelf and 1484 ± 467 ng g^{-1} in the central Arctic Ocean (Tab. S2). The Hg_{SPM} concentrations in the central Arctic Ocean were comparable to those measured by Lamborg et al. (2016) in the North Atlantic (240 - 1080 ng g^{-1}), but 4 to 30 times higher than ones Soerensen et al. (2016) for their model. From Hg_{SPM} and dissolved Hg observations we calculated K_d for each station. The K_d values range from 1.2 x 10^6 to 1.6 x 10^7 L kg^{-1}. Our lowest K_d values are one order of magnitude higher than the value applied by Fisher et al. (2012) in their model (1.1 x 10^5 L kg^{-1}), and 3 times higher than those determined in the North Atlantic (4.5 x 10^6 L kg^{-1}, Lamborg et al., 2016, Tab. S2). Our Hg_{SPM} and K_d values suggest that previous studies may have underestimated Hg export fluxes.

To test this, we used the ^{234}Th /^{238}U deficit measurements to quantify the Hg export flux in the Arctic Ocean. Several studies have employed the ^{234}Th proxy to estimate the particulate flux of trace metals and other compounds (Gustafsson et al., 1997a, Gustafsson et al., 1997b, Dulaquais et al., 2014, Weinstein et al., 2005, Hayes et al., 2018, Black et al., 2019). Here we apply for the first time the radionuclide pair ^{234}Th /^{238}U, combined with pHg /^{234}Th ratios, to estimate the downward Hg export flux. The half-life of ^{234}Th is 24.1 days and it is highly particle reactive with K_d values (~10^6 - 10^7, IAEA, 1985) similar to those of Hg in oxygenated sea water (Lamborg et al., 2016). The relatively short half-life of ^{234}Th makes it a suitable tracer to examine biologically mediated temporal changes in POC production and export, by using the POC/^{234}Th ratio in the particles to convert the ^{234}Th export flux to POC export flux (Coale et al., 1985, Buesseler et al., 1992). Similarly, here we measured the pHg /^{234}Th ratios on filtered particulates (1 - 51 or 53 µm) to convert the ^{234}Th flux to the pHg

flux, assuming that the pHg /^{234}Th ratios in those particles are equivalent to the ratios on the sinking particles driving pHg export. We chose to sample at 100 m depth within the halocline, well below the polar mixed layer (typically 20 m) and above the Atlantic-sourced waters (typically 150 - 700 m depth). The particulate ^{234}Th activities measured during the GN04 and GN01 cruises averaged 0.24 ± 0.16 dpm L^{-1} (n = 19, range 0.067 - 0.76 dpm L^{-1}, Tab. S2). We calculated ^{234}Th export flux at 100 m depth, which ranged between -300 ± 100 and 569 ± 207 dpm m^{-2} d^{-1} in the central Arctic Ocean and between 221 ± 175 and 700 ± 100 dpm m^{-2} d^{-1} on the shelf (Tab. S2). Negative values are considered to be negligible and equal to zero, which might be caused by remineralization, lateral advection (Savoye et al., 2004, Maiti et al., 2010) and/or inputs of ^{234}Th -enriched ice algae (Rodriguez y Baena et al., 2008). Low (or negligible) ^{234}Th export fluxes are common in the Arctic Ocean (Roca Marti et al., 2016) particularly at the end of summer when the cruises took place, due to low productivity and a community structure that does not promote efficient export. The average pHg /^{234}Th ratio was 0.48 ± 0.31 pmol dpm^{-1} (n = 19, range 0.072 - 1.05 pmol dpm^{-1}, Tab. S2). Based on the measured pHg /^{234}Th ratios, we estimated the Hg export fluxes at each station, which were lower in the permanently ice-covered central Arctic Ocean and higher over the outer shelf (Tab. S2). Applying the average pHg /^{234}Th ratio measured during GN01 and GN04 to the ^{234}Th fluxes reported in the current and by previous studies (Amiel et al., 2002, Coppola et al., 2002, Chen et al., 2003, Qiang et al., 2005, Lalande et al., 2007, Amiel et al., 2008, Lalande et al., 2008, Cai et al., 2010, Roca-Martí et al., 2016) we estimated the Hg export fluxes below 100 m depth for different locations in the central Arctic Ocean and outer shelf zones (Fig.1).

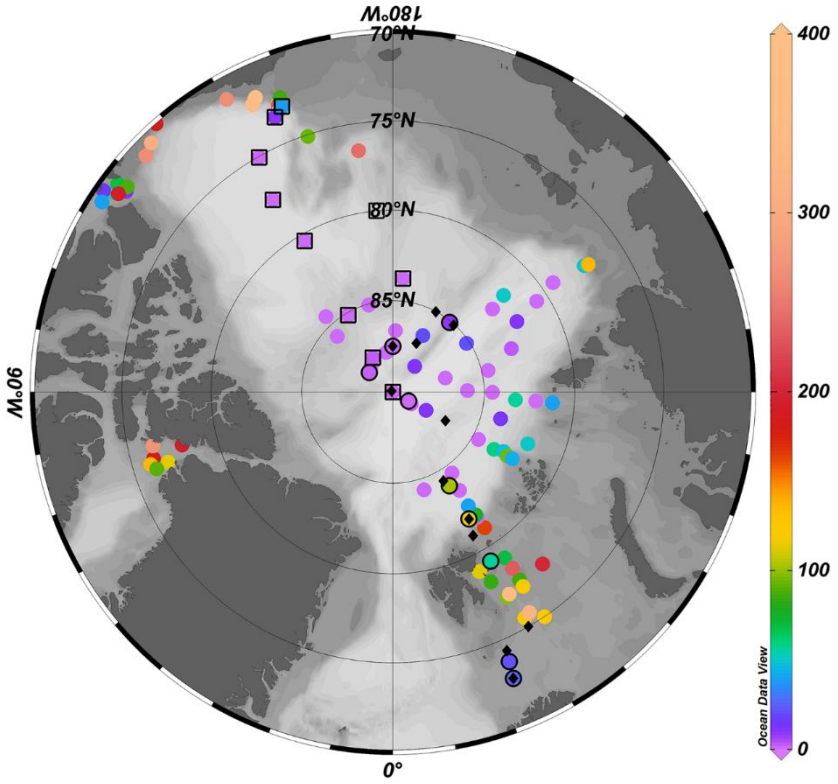

Fig. 1. Particulate Hg export fluxes at 100 m (pmol m^{-2} day^{-1}) derived from the ^{234}Th approach and the pHg /^{234}Th ratios from this study. Negative fluxes were considered equal to zero. Black circles and squares indicate stations from the GN04 and GN01 cruises, respectively. Black diamonds indicate stations from GN04 where sediment cores were collected. The other data points have been calculated using previously published ^{234}Th fluxes (Amiel et al., 2002, Coppola et al., 2002, Chen et al., 2003, Qiang et al., 2005, Lalande et al., 2007, Amiel et al., 2008, Lalande et al., 2008, Cai et al., 2010, Roca-Martí et al., 2016) and the average pHg /^{234}Th ratio obtained in this study.

The lowest pHg export fluxes were found in the permanently ice-covered central Arctic Ocean (average 95 ± 195 pmol m^{-2} d^{-1}, n = 49) while the highest were found in the outer shelf (average 635 ± 480 pmol m^{-2} d^{-1}, n = 50, Fig. 1). Our pHg export flux estimates for the central Arctic Ocean are comparable to observations in the Pacific Ocean based on

sediment trap deployments (157 ± 48 pmol m^{-2} d^{-1}, Munson et al., 2015). However, we observe higher pHg export flux on the productive outer shelf. Our assessment might be slightly biased by seasonal and long term variability, because some of the used literature ^{234}Th export fluxes were obtained during different seasons and years. Similar to our study, some of the previously reported values indicated negligible ^{234}Th export fluxes (Amiel et al., 2002, Coppola et al., 2002, Chen et al., 2003, Qiang et al., 2005, Lalande et al., 2007, Amiel et al., 2008, Lalande et al., 2008, Cai et al., 2010, Roca-Martí et al., 2016).

To estimate the annual export flux of Hg, we used a primary production period of 85 days for the central Arctic Ocean and 190 days for the outer shelf (Strass et al., 1996, Niebauer et al., 1999) and surface areas for the central Arctic Ocean and the outer shelf of 5 x 10^6 km^2 and 3 x 10^6 km^2, respectively. Based on this assumption we estimated that 8 ± 17 Mg y^{-1} of Hg are exported below 100 m depth in the central Arctic Ocean and 73 ± 55 Mg y^{-1} over the outer shelf (Fig. 2). The fact that most of the Hg export takes place over the outer shelf is likely related to the enhanced primary productivity compared to the central arctic basin waters (Sakahaug et al., 2004). Several studies already reported high uncertainties of ^{234}Th-derived C and trace-metal fluxes (Le Moigne et al., 2013, Puigcorbé et al, 2017, Black et al., 2019). We estimated a lower boundary for the pHg export flux from surface water with 81 ± 58 Mg y^{-1}. If we assume that fluxes on the inner shelf (< 100 m depth), which represents about 25% of the Arctic Ocean surface and receives direct Hg and nutrients inputs via river runoff and coastal erosion (Soerensen et al., 2016, Sonke et al., 2018), were similar to those of the outer shelf, extrapolated the inner shelf, annual flux for the entire Arctic Ocean is about 156 Mg y^{-1}.

Settling particles are remineralized during their downward flux and only a small portion is finally buried in marine sediments (Heimbürger et al., 2012) To check how this affects Hg export flux we measured pHg concentrations in sediments collected during the

GN04 cruise on the outer shelf and central Arctic Ocean (Fig. 1). We used our data and previous pHg observations (upper 0.5 – 2 cm, Gobeil et al., 1999, Trefry et al., 2003, Hare et al., 2010, Fox et al., 2014, Canário et al., 2014, Tab. S3) to estimate the net Hg burial rates. Based on sedimentation rates typically found in the Arctic Ocean (0.03 mm y^{-1}) and for the open ocean and outer shelf (0.3 mm y^{-1}) following Soerensen et al. (2016), we calculated average Hg burial rates of 11 ± 8 and 51 ± 35 pmol m^{-2} d^{-1}, respectively. Considering the surface area of the central Arctic Ocean and outer shelf with 5 x 10^6 and 3 x 10^6 km^2, respectively, we estimated Hg burial rates of 4 ± 3 Mg y^{-1} in the central Arctic Ocean and 12 ± 7 Mg y^{-1} in the deep shelf (Tab. S3). Our new estimates are slightly lower than those by Soerensen et al. (2016) (3 and 25 Mg y^{-1}, respectively). In the absence of pHg observations on the inner shelf, our Hg burial rate of 16 ± 10 Mg y^{-1} for the Arctic Ocean is a lower boundary. If we were to compare our results (51 ± 35 pmol m^{-2} d^{-1}) to another semi-enclosed basin, the Mediterranean Sea, with sedimentation rates (0.4 mm y^{-1}) similar to the arctic outer shelf (0.3 mm y^{-1}), we find lower Hg burial rates than 115 pmol m^{-2} d^{-1} (Heimbürger et al., 2012). The high range of observed sedimentation rates, 0.0025 - 0.05 mm y^{-1} for the central Arctic Ocean and 0.1 - 2.5 mm y^{-1} for the shelf (Pirtle-Levy et al., 2009, Polyak et al., 2011, Polyak et al., 2011) also results in a high uncertainty in the Hg burial rates estimates.

We used our new estimates of pHg downward export and the Hg burial fluxes combined with current observations and modelling studies (Soerensen et al., 2016, Sonke et al., 2018, Petrova et al., 2020) to refine our understanding of the Hg cycle in the Arctic Ocean (Fig. 2). Based on our Hg observations on SPM and sediments, we calculate that 5.6 ± 2.9% of the exported pHg from the upper 100 m depth is ultimately buried in the central Arctic sediments. Most of the pHg downward flux is remineralized below 100 m depth which is also suggested by the $^{234}Th/^{238}U$ profiles (Puigcorbé pers. comm., data not shown here). We hypothesize that pHg exported below 100 m depth may contribute to the shallow production

MeHg in the Arctic Ocean (Wang et al., 2012, Wang et al., 2018, Heimbürger et al., 2015, Agather et al., 2019). Post depositional diagenetic processes lead to epibenthic mobilization of dissolved Hg species to overlaying sea water. Heimbürger et al. (2012) found that epibenthic mobilization of Hg can explain 73% of the observed difference between water column export flux and Hg burial. Our study could not address the possible influence of nycthemeral zooplankton dynamics, convective SPM and diffusive fluxes. Cascading processes, which take place on the shelf by the downwelling of waters (Roeske et al., 2012) may also be an important pathway for pHg and 234Th displacement from shallow to deep waters.

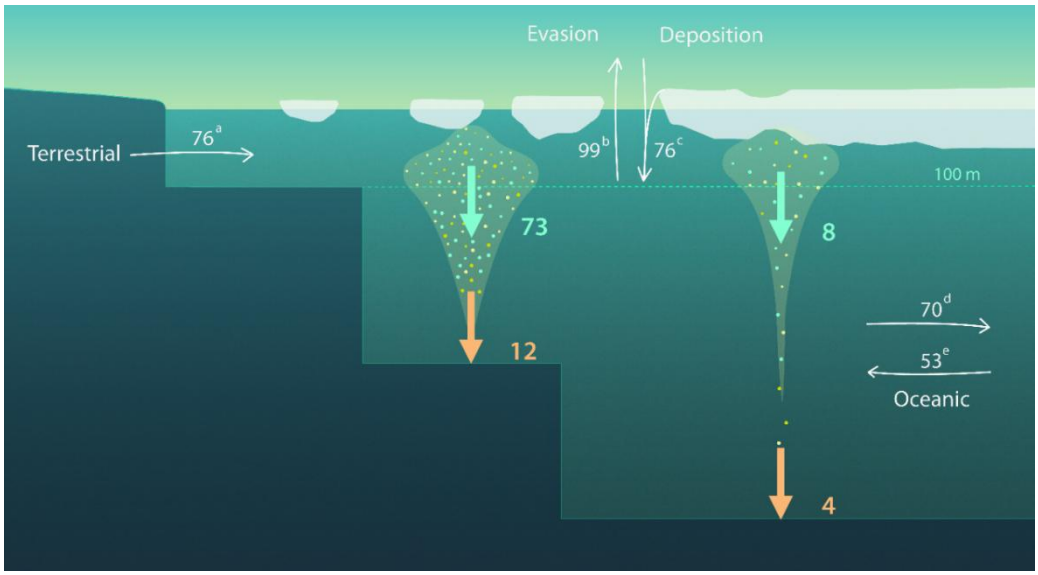

Fig. 2: Mass balance of Hg in the Arctic Ocean with fluxes (Mg y^{-1}) components estimated in this study: export fluxes at 100 m (labelled as green arrows) and the net burial fluxes (labelled as orange arrows) combined with fluxes described by Soerensen et al. (2016) (a, b, c and d), Sonke et al. (2018) (a), Petrova et al. (2020) (d and e).

About 76 Mg y^{-1} of Hg have been suggested to be transported to the Arctic shelves by rivers or sourced from coastal erosion (Soerensen et al., 2016, Sonke et al., 2018). The high sensitivity of the Arctic to climate change can perturb Arctic Hg cycling, increasing land to

ocean Hg export fluxes since permafrost thawing and extreme weather events are expected to deliver important amounts of Hg to Arctic Ocean (Schuster et al., 2018). In addition, the increase of the open water season due to ice-retreat is leading to an increase of net primary production (Arrigo et al., 2015) enhancing also Hg scavenging and downward export, which would reduce the amount of Hg available for MeHg production. However, shift to small-sized phytoplankton, may lead to increased MeHg production (Heimbürger et al., 2015). Only continued seasonal and long term arctic surveys will allow building a first time series and make coherent future projections.

About half of the Arctic shelf is shallower than 100 m (inner shelf), and could not be addressed by our study. We can only provide approximate pHg export fluxes below 100 m depth for the outer shelf and the central Arctic Ocean. The use of pHg /^{234}Th ratio in particles to obtain Hg export flux should be further developed and expanded to other oceans. In particular, future research should address the spatial and temporal variability of the pHg /^{234}Th ratio considering biogeochemical regions and seasonality. Ongoing climate change impacts to the Arctic Ocean ecosystem should also be assessed, including changes in sea ice cover, particle and nutrient supply, primary productivity, and hydrological circulations will likely impact pHg export and overall Hg budget in the Arctic Ocean.

Methods

We used pHg from the GN01 cruise for which information on the measurements details are given by Agather et al. (2019). We obtained the data set upon request from Alison Agather by personal email and should become available on https://www.bco-dmo.org/dataset/738307. Particles were collected using McLane *in situ* pumps (LV08) equipped with a pre-filter (screen) of 51 or 53 µm pore size (for GN01 and GN04, respectively) followed by a pre-combusted QMA filter from where the samples for this study were collected (i.e., particle size sampled 1 - 51 or53 µm). For both cruises, particulate ^{234}Th

and pHg were measured from the exact same filter. Punches (25 mm) were subsampled from each filter for particulate ^{234}Th, dried overnight at 50°C and counted on board and recounted again 6 months later for background corrections. After the second counting, POC content was analyzed in the same filters with an EuroVector Elemental Analyzer (Euroanalysator EA).

During the GN04 cruise pHg the remainder of the filters were kept frozen at -20°C until analyses for pHg. Twelve sediment cores were recovered using the trace metal clean NIOZ minicorer. Sediment cores were sliced every 5 mm using a Plexiglas spatula. Only the upper 5 mm were considered for the estimation of Hg burial rates. The sediment samples were kept frozen at -20°C until analyses for pHg. All samples were freeze-dried (Christ Gamma 1-16 LSCplus) and 25 mm diameter punch-out samples were analysed using a CV-AAS (LECO AMA 254) equipped with a low Hg optical cell. The limit of detection, estimated as three times standard deviation of the blank samples, was 1.2 pg, which was equivalent to about 0.0001 pM considering the filtered amount of sea water (289 - 599 L).

Total ^{234}Th activities were determined from 4 L of sea water collected at 18 - 20 depths (GN04) or 10 - 15 depths (GN01) in the upper ~ 400 m of the water column. Replicates of deep samples (GN04: 3000 m, GN01: 2000 m) were collected for calibration purposes (van der Loeff et al., 2006). The samples were processed following the MnO_2 co-precipitation technique (Buesseler et al., 2001) using ^{230}Th as a chemical yield tracer (Pike et al., 2005). The counting was done on board using low background beta counters and measured again 6 months later for background quantification, as per particulate ^{234}Th samples. Recoveries for ^{234}Th were determined on all filters by inductively coupled plasma mass spectrometry with an average recovery of 0.87 ± 0.03 (n = 225, GN04).

Acknowledgements

The authors would like to thank the chief scientists Ursula Schauer, Dave Kadko and William Landing; Captains, officers and crew of the FS Polarstern and the USCGC Healy. We thank the CNRS Chantier Arctique Français funding via the Pollution in the Arctic System project, European Research Council (ERC-2010-StG_20091028) to JES and the AXA Research Fund to LEHB (postdoc grant Levering Knowledge Gaps To Understand And Anticipate Risk From Methylmercury Exposure; and outreach grant Arctic Mediterranean Mercury). We also thank a NASA Earth and Space Science Fellowship Program grant (NNX13AP31H) and the National Science Foundation (OCE- 1458305) funding to EEB. We are thankful to Sandra Gdaniec for her support with the *in situ* pump sampling and to Walter Geibert for the thorium recovery analyses. The IAEA is grateful for the support provided to its Environment Laboratories by the Government of the Principality of Monaco. PM acknowledges the support of the Generalitat de Catalunya (MERS 2017 SGR – 1588). This work contributes to the ICTA Unit of Excellence (MinECo, MDM2015-0552). We also thank Itziar Tesán for the support with a graphical design.

References

Agather, A.M., Bowman, K.L., Lamborg, C.H., Hammerschmidt, C.R., 2019. Distribution of mercury species in the Western Arctic Ocean (U.S. GEOTRACES GN01). Marine Chemistry 216, 103686

Amiel, D., Cochran, J. K., Hirschberg, D. J., 2002. 234Th/238U Disequilibrium as an Indicator of the Seasonal Export Flux of Particulate Organic Carbon in the North Water. Deep Sea Research Part II: Topical Studies in Oceanography, 49 (22–23), 5191–5209

Amiel, D., Cochran, J. K., 2008. Terrestrial and Marine POC Fluxes Derived from 234 Th Distributions and δ 13 C Measurements on the Mackenzie Shelf. Journal of Geophysical Research, 113 (C3)

Arrigo, K.R., van Dijken, G.L., 2015. Continued increases in Arctic Ocean primary production. Progress in Oceanography 136, 60–70

Black, E.E., Lam, P.J., Lee, J. - M., Buesseler, K.O., 2018. Insights from the ^{238}U-^{234}Th Method into the Coupling of Biological Export and the Cycling of Cadmium, Cobalt, and Manganese in the Southeast Pacific Ocean. Global Biogeochemical Cycles 33, 15-36

Bowman, K.L., Hammerschmidt, C.R., Lamborg, C.H., Swarr, G., 2015. Mercury in the North Atlantic Ocean: The U.S. GEOTRACES zonal and meridional sections. Deep Sea Research Part II: Topical Studies in Oceanography 116, 251–261

Buesseler, K.O., Bacon, M.P., Kirk Cochran, J., Livingston, H.D., 1992. Carbon and nitrogen export during the JGOFS North Atlantic Bloom experiment estimated from 234Th: 238U disequilibria. Deep Sea Research Part A. Oceanographic Research Papers 39, 1115–1137

Buesseler, K.O., Benitez-Nelson, C., Rutgers van der Loeff, M., Andrews, J., Ball, L., Crossin, G., Charette, M.A., 2001. An Intercomparison of Small- and Large-Volume Techniques for Thorium-234 in Seawater. Marine Chemistry, 74 (1), 15–28

Burt, A. E. 2012. Mercury uptake and dynamics in sea ice algae, phytoplankton and grazing copepods from a Beaufort Sea Arctic marine food web. Univ. of Manitoba. 92 pp

Cai, P., Rutgers van der Loeff, M., Stimac, I., Nöthig, E.-M., Lepore, K., Moran, S. B., 2010. Low Export Flux of Particulate Organic Carbon in the Central Arctic Ocean as Revealed by 234Th:238U Disequilibrium. J. Geophys. Res.: Oceans, 115(C10), C10037

Canário, J., Poissant, L., Pilote, M., Blaise, C., Constant, P., Férard, J.-F., Gagné, F., 2014. Toxicity survey of Canadian Arctic marine sediments. Journal of Soils and Sediments 14, 196–203

Chen, M., Huang, Y., Cai, P., Guo, L., 2003. Particulate Organic Carbon Export Fluxes in The Canada Basin and Bering Sea as Derived from 234Th/238U Disequilibria. ARCTIC, 56 (1)

Coale, K.H., Bruland, K.W., 1985. 234Th:238U disequilibria within the California Current. Limnology and Oceanography 30, 22–33

Coppola, L., Roy-Barman, M., Wassmann, P., Mulsow, S., Jeandel, C., 2002. Calibration of Sediment Traps and Particulate Organic Carbon Export Using 234 Th in the Barents Sea. Marine Chemistry, 80 (1), 11–26

Cossa, D., Heimbürger, L.E., Pérez, F.F., García-Ibáñez, M.I., Sonke, J.E., Planquette, H., Lherminier, P., Boutorh, J., Cheize, M., Menzel Barraqueta, J.L., Shelley, R., Sarthou, G., 2018. Mercury distribution and transport in the North Atlantic Ocean along the GEOTRACES-GA01 transect. Biogeosciences 15, 2309–2323

Dietz, R., Sonne, C., Basu, N., Braune, B., O'Hara, T., Letcher, R.J., Scheuhammer, T., Andersen, M., Andreasen, C., Andriashek, D., Asmund, G., Aubail, A., Baagøe, H., Born, E.W., Chan, H.M., Derocher, A.E., Grandjean, P., Knott, K., Kirkegaard, M., Krey, A., Lunn, N., Messier, F., Obbard, M., Olsen, M.T., Ostertag, S., Peacock, E., Renzoni, A., Rigét, F.F., Skaare, J.U., Stern, G., Stirling, I., Taylor, M., Wiig, Ø., Wilson, S., Aars, J., 2013. What are

the toxicological effects of mercury in Arctic biota? Science of The Total Environment 443, 775–790

Dulaquais, Gabriel, Boye, M., Middag, R., Owens, S., Puigcorbé, V., Buesseler, K., Masqué, P., de Baar, H.J.W., Carton, X., 2014. Contrasting biogeochemical cycles of cobalt in the surface western Atlantic Ocean: Surface biogeochemical cycles of cobalt. Global Biogeochemical Cycles 28, 1387–1412

Dudarev, A., Chupakhin, V., Vlasov, S., Yamin-Pasternak, S., 2019. Traditional Diet and Environmental Contaminants in Coastal Chukotka III: Metals. International Journal of Environmental Research and Public Health 16, 699

Fisher, J.A., Jacob, D.J., Soerensen, A.L., Amos, H.M., Steffen, A., Sunderland, E.M., 2012. Riverine source of Arctic Ocean mercury inferred from atmospheric observations. Nature Geoscience 5, 499–504

Fox, A.L., Hughes, E.A., Trocine, R.P., Trefry, J.H., Schonberg, S.V., McTigue, N.D., Lasorsa, B.K., Konar, B., Cooper, L.W., 2014. Mercury in the northeastern Chukchi Sea: Distribution patterns in seawater and sediments and biomagnification in the benthic food web. Deep Sea Research Part II: Topical Studies in Oceanography 102, 56–67

Gobeil, C., Macdonald, R.W., Smith, J.N., 1999. Mercury Profiles in Sediments of the Arctic Ocean Basins. Environmental Science & Technology 33, 4194–4198

Graydon, J.A., Emmerton, C.A., Lesack, L.F.W., Kelly, E.N., 2009. Mercury in the Mackenzie River delta and estuary: Concentrations and fluxes during open-water conditions. Science of The Total Environment 407, 2980–2988

Gustafsson, Ö., Gschwend, P.M., Buesseler, K.O., 1997a. Settling Removal Rates of PCBs into the Northwestern Atlantic Derived from ^{238}U− ^{234}Th Disequilibria. Environmental Science & Technology 31, 3544–3550

Gustafsson, Ö., Gschwend, P.M., Buesseler, K.O., 1997b. Using 234Th disequilibria to estimate the vertical removal rates of polycyclic aromatic hydrocarbons from the surface ocean. Marine Chemistry 57, 11–23

Hare, A.A., Stern, G.A., Kuzyk, Z.Z.A., Macdonald, R.W., Johannessen, S.C., Wang, F., 2010. Natural and Anthropogenic Mercury Distribution in Marine Sediments from Hudson Bay, Canada. Environmental Science & Technology 44, 5805–5811

Hayes, C.T., Black, E.E., Anderson, R.F., Baskaran, M., Buesseler, K.O., Charette, M.A., Cheng, H., Cochran, J.K., Edwards, R.L., Fitzgerald, P., Lam, P.J., Lu, Y., Morris, S.O., Ohnemus, D.C., Pavia, F.J., Stewart, G., Tang, Y., 2018. Flux of Particulate Elements in the North Atlantic Ocean Constrained by Multiple Radionuclides. Global Biogeochemical Cycles 32, 1738–1758

Heimbürger, L.E., Cossa, D., Thibodeau, B., Khripounoff, A., Mas, V., Chiffoleau, J.-F., Schmidt, S., Migon, C., 2012. Natural and anthropogenic trace metals in sediments of the Ligurian Sea (Northwestern Mediterranean). Chemical Geology 291, 141–151

Heimbürger, L.E., Sonke, J. E., Cossa, D., Point, D., Lagane, C., Laffont, L., Galfond, B. T., Nicolaus, M., Rabe, B., Van Der Loeff, M. R., 2015. Shallow methylmercury production in the marginal sea ice zone of the central Arctic Ocean. Sci. Rep. 5, 10318

IAEA, 1985. Sediment Kd's and concentration factors for radionuclides in the marine environment. Technical Reports Series 247. Vienna, Austria.

Kraft, A., Bauerfeind, E., Nöthig, E.-M., Klages, M., Beszczynska-Möller, A., Bathmann, U.V., 2013. Amphipods in sediment traps of the eastern Fram Strait with focus on the life-history of the lysianassoid Cyclocaris guilelmi. Deep Sea Research Part I: Oceanographic Research Papers 73, 62–72

Lalande, C., Lepore, K., Cooper, L. W., Grebmeier, J. M., Moran, S. B., 2007. Export Fluxes of Particulate Organic Carbon in the Chukchi Sea: A Comparative Study Using 234Th/238U Disequilibria and Drifting Sediment Traps. Marine Chemistry, 103 (1–2), 185–196

Lalande, C., Moran, S. B., Wassmann, P., Grebmeier, J. M., Cooper, L. W., 2008. 234Th-Derived Particulate Organic Carbon Fluxes in the Northern Barents Sea with Comparison to Drifting Sediment Trap Fluxes. Journal of Marine Systems, 73 (1–2), 103–113

Lamborg, C.H., Hammerschmidt, C.R., Bowman, K.L., 2016. An examination of the role of particles in oceanic mercury cycling. Philosophical Transactions of the Royal Society A: Mathematical, Physical and Engineering Sciences 374, 20150297

Leitch, D.R., Carrie, J., Lean, D., Macdonald, R.W., Stern, G.A., Wang, F., 2007. The delivery of mercury to the Beaufort Sea of the Arctic Ocean by the Mackenzie River. Science of The Total Environment 373, 178–195

Le Moigne, F. A. C., Henson, S. A., Sanders, R. J., Madsen, E., 2013. Global Database of Surface Ocean Particulate Organic Carbon Export Fluxes Diagnosed from the 234Th Technique.Earth System Science Data, 5(2), 295−304

Lam, P. J., 2020. Size-fractionated major and minor particle composition and concentration from the US GEOTRACES Arctic cruise (HLY1502) on USCGC Healy from August to October 2015. Biological and Chemical Oceanography Data Management Office (BCO-DMO), Dataset version 2020-04-01

Lim, A. G., Jiskra, M., Sonke, J. E., Loiko, S. V., Kosykh, N., Pokrovsky, O. S., 2020. A revised northern soil Hg pool, based on western Siberia permafrost peat Hg and carbon observations, Biogeosciences Discuss

Macdonald, R.W., Thomas, D.J., 1991. Chemical interactions and sediments of the western Canadian arctic shelf. Continental Shelf Research 11, 843–863

Maiti, K., Benitez-Nelson, C.R., Buesseler, K.O., 2010. Insights into particle formation and remineralization using the short-lived radionuclide, Thorium-234: particle remineralization using Th-234. Geophysical Research Letters 37

Mason, R.P., Fitzgerald, W.F., 1993. The distribution and biogeochemical cycling of mercury in the equatorial Pacific Ocean. Deep Sea Research Part I: Oceanographic Research Papers 40, 1897–1924

Mason, R.P., Rolfhus, K.R., Fitzgerald, W.F., 1998. Mercury in the North Atlantic. Marine Chemistry 61, 37–53

Munson, K.M., Lamborg, C.H., Swarr, G.J., Saito, M.A., 2015. Mercury species concentrations and fluxes in the Central Tropical Pacific Ocean: Central Pacific mercury. Global Biogeochemical Cycles 29, 656–676

Niebauer, H.J., 1999. An update on the climatology and sea ice of the Bering Sea, in: The Bering Sea: A Summary of Physical, Chemical and Biological Characteristics and a Synopsis of Research.

Outridge, P.M., Macdonald, R.W., Wang, F., Stern, G.A., Dastoor, A.P., 2008. A mass balance inventory of mercury in the Arctic Ocean. Environmental Chemistry 5, 89

Petrova, M.V., Krisch, S., Lodeiro, P., Valk, O., Dufour, A., Rijkenberg, M.J.A., Takamasa, Achtenberg, E.P., Rabe, B., van der Loeff, M.R., Hamelin, B., Sonke, J.E., Heimbürger-Boavida L.E., 2020. Arctic Ocean exports methylmercury to the Atlantic Ocean. Marine Chemistry, 225, 103855

Pike, S.M., Buesseler, K.O., Andrews, J., Savoye, N., 2005. Quantification of 234 Th recovery in small volume seawater samples by inductively coupled plasma-mass spectrometry. Journal of Radioanalytical and Nuclear Chemistry 263, 355–360

Pirtle-Levy, R., J. M. Grebmeier, L. W. Cooper, I. L. Larsen., 2009. Chlorophyll-a in Arctic sediments implies long persistence of algal pigments, Deep Sea Research, Part II,56(17), 1326–1338

Polyak, L., Bischof, J., Ortiz, J.D., Darby, D.A., Channell, J.E.T., Xuan, C., Kaufman, D.S., Løvlie, R., Schneider, D.A., Eberl, D.D., Adler, R.E., Council, E.A., 2009. Late Quaternary stratigraphy and sedimentation patterns in the western Arctic Ocean. Global and Planetary Change 68, 5–17

Polyak, L., Jakobsson, M. 2011. Quaternary sedimentation in the Arctic Ocean: Recent advances and further challenges. Oceanography 24(3), 52–64

Pućko, M., Burt, A., Walkusz, W., Wang, F., Macdonald, R.W., Rysgaard, S., Barber, D.G., Tremblay, J.-É., Stern, G.A., 2014. Transformation of Mercury at the Bottom of the Arctic Food Web: An Overlooked Puzzle in the Mercury Exposure Narrative. Environmental Science & Technology 48, 7280–7288

Puigcorbé, V., Roca-Martí, M., Masqué, P., Benitez-Nelson, C., Rutgers van der Loeff, M., Bracher, A., Moreau, S., 2017. Latitudinal Distributions of Particulate Carbon Export across the North Western Atlantic Ocean Deep Sea Res., Part I, 129, 116−130

Qiang, M., Min, C., Yusheng, Q., Yanping, L.I., 2005. Regional estimates of POC export flux derived from thorium-234 in the western Arctic Ocean. 海洋学报 (中文版), 24(6), 97–108

Roca-Martí, M., Puigcorbé, V., Rutgers van der Loeff, M.M., Katlein, C., Fernández-Méndez, M., Peeken, I., Masqué, P., 2016. Carbon export fluxes and export efficiency in the central Arctic during the record sea-ice minimum in 2012: a joint ^{234}Th/^{238}U and ^{210}Po/^{210}Pb study: POC fluxes in the central Arctic in 2012. Journal of Geophysical Research: Oceans 121, 5030–5049

Rodriguez y Baena, A.M., Boudjenoun, R., Fowler, S.W., Miquel, J.C., Masqué, P., Sanchez-Cabeza, J.-A., Warnau, M., 2008. 234Th-based carbon export during an ice-edge bloom: Sea-ice algae as a likely bias in data interpretation. Earth and Planetary Science Letters 269, 596–604

Roeske, T., Middag, R., Bakker, K., Rutgers v. d. Loeff, M., 2012. Deep water circulation and shelf water inputs to the Arctic Ocean by dissolved Ba. Marine Chemistry 132-133, 56-67

Sakshaug, E., 2004. Primary and Secondary Production in the Arctic Seas, in: The Organic Carbon Cycle in the Arctic Ocean. pp. 57–81

Savoye, N., Buesseler, K.O., Cardinal, D., Dehairs, F., 2004. ^{234} Th deficit and excess in the Southern Ocean during spring 2001: Particle export and remineralization: S.O. particle export and remineralization. Geophysical Research Letters 31

Schroeder, W.H., Anlauf, K.G., Barrie, L.A., Lu, J.Y., Steffen, A., Schneeberger, D.R., Berg, T., 1998. Arctic springtime depletion of mercury. Nature 394, 331–332

Schuster, P.F., Schaefer, K.M., Aiken, G.R., Antweiler, R.C., Dewild, J.F., Gryziec, J.D., Gusmeroli, A., Hugelius, G., Jafarov, E., Krabbenhoft, D.P., Liu, L., Herman- Mercer, N., Mu, C., Roth, D.A., Schaefer, T., Striegl, R.G., Wickland, K.P., Zhang, T., 2018. Permafrost Stores a Globally Significant Amount of Mercury. Geophysical Research Letters 45, 1463–1471

Soerensen, A.L., Jacob, D.J., Schartup, A.T., Fisher, J.A., Lehnherr, I., St. Louis, V.L., Heimbürger, L.-E., Sonke, J.E., Krabbenhoft, D.P., Sunderland, E.M., 2016. A mass budget for mercury and methylmercury in the Arctic Ocean: Arctic Ocean Hg and MeHg mass budget. Global Biogeochemical Cycles 30, 560–575

Sonke, J.E., Teisserenc, R., Heimbürger-Boavida, L.-E., Petrova, M.V., Marusczak, N., Le Dantec, T., Chupakov, A.V., Li, C., Thackray, C.P., Sunderland, E.M., Tananaev, N.,

Pokrovsky, O.S., 2018. Eurasian river spring flood observations support net Arctic Ocean mercury export to the atmosphere and Atlantic Ocean. Proceedings of the National Academy of Sciences 115, E11586–E11594

Strass, V.H., Nöthig, E.-M., 1996. Seasonal shifts in ice edge phytoplankton blooms in the Barents Sea related to the water column stability. Polar Biology, 16, 409–422

Trefry, J.H., Rember, R.D., Trocine, R.P., Brown, J.S., 2003. Trace metals in sediments near offshore oil exploration and production sites in the Alaskan Arctic. Environmental Geology 45, 149–160

van der Loeff, M.R., Sarin, M.M., Baskaran, M., Benitez-Nelson, C., Buesseler, K.O., Charette, M., Dai, M., Gustafsson, Ö., Masque, P., Morris, P.J., Orlandini, K., Rodriguez y Baena, A., Savoye, N., Schmidt, S., Turnewitsch, R., Vöge, I., Waples, J.T., 2006. A review of present techniques and methodological advances in analyzing 234Th in aquatic systems. Marine Chemistry 100, 190–212

Wang, F., Macdonald, R.W., Armstrong, D.A., Stern, G.A., 2012. Total and Methylated Mercury in the Beaufort Sea: The Role of Local and Recent Organic Remineralization. Environmental Science & Technology 46, 11821–11828

Wang, K., Munson, K.M., Beaupré-Laperrière, A., Mucci, A., Macdonald, R.W., Wang, F., 2018. Subsurface seawater methylmercury maximum explains biotic mercury concentrations in the Canadian Arctic. Scientific Reports 8

Weinstein, S.E., Moran, S.B., 2005. Vertical flux of particulate Al, Fe, Pb, and Ba from the upper ocean estimated from 234Th/238U disequilibria. Deep Sea Research Part I: Oceanographic Research Papers 52, 1477–1488